

NUMERICAL ANALYSIS OF SOLAR THERMO-CHEMICAL REACTOR

Prince Priyadarshi¹, Saumitra Kumar Sharma²

¹Reserch Scholar, ²Assistant Professor

Department of mechanical engineering

Oriental College of Technology, Bhopal (M.P.) India

Abstract: Due to advances in its effectiveness and efficiency, solar thermal energy is becoming increasingly attractive as a renewable energy source. Efficient energy storage, however, is a key limiting factor on its further development and adoption. The solar thermo chemical fuel production pathway as an attractive option for the decarbonization of the transportation sector is investigated. In this paper, the main objective is to study the effect of various parameters on the working of thermo chemical reactor. The parameters which are studied here are porosity, velocity and length of the porous material. In the present study NX11 software is used for CAD modeling. And ANSYS is the software used for modelling as well as for testing the products durability, temperature distribution in product and the movement of fluid under various boundary conditions. The results of all seven cases are also discussed. These include solar water heating, which comprise thermo syphon, integrated collector storage, direct and indirect systems and air systems, space heating and cooling, which comprise, space heating and service hot water, air and water systems and heat pumps, refrigeration, industrial process heat, which comprise air and water systems and steam generation systems, desalination, thermal power systems, which comprise the parabolic trough, power tower and dish systems, solar furnaces, and chemistry applications. As can be seen solar energy systems can be used for a wide range of applications and provide significant benefits, therefore, they should be used whenever possible.

Keywords: Solar thermal energy, porosity, thermo chemical fuel, meshing, boundary condition.

INTRODUCTION

A solar thermo-chemical reactor is modeled and analyzed for the solar thermal dissociation of zinc oxide into zinc and oxygen involved in the thermo-chemical cycle for hydrogen production. Solar thermochemical processes are suitable for production of fuels, in which solar energy is stored in form of chemical bonds, and chemical commodities for industrial, agricultural, and other applications. Examples of solar thermochemical processes for fuel production include upgrading fossil fuels and biomass, thermal reduction of metal oxides, and direct water thermolysis. Solar thermal energy is a promising source of process heat for a variety of thermochemical processes, from splitting water to produce hydrogen, to upgrading of carbonaceous feed stocks, to providing process heat for CO₂ capture. Most directly irradiated solar thermochemical systems must deal with these

transients by varying the production rate and they possibly have a change in product mixture or quality due to changing temperature. Solar thermal storage can address transients, but usually add several energy conversion steps between the solar radiation and the chemical reaction.

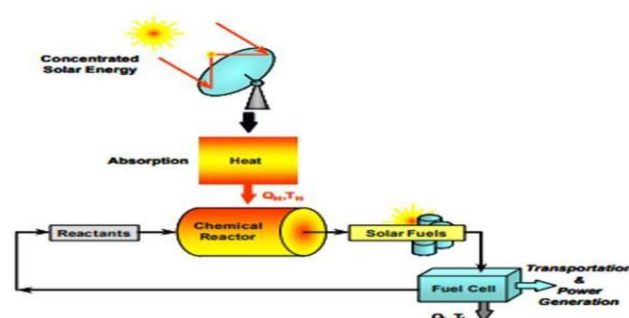


Figure 1 Working of solar thermochemical reactor (Steinfeld & Palumbo, 2003)

From a fundamental perspective, using sunlight as a source of thermal energy provides advantages over photo catalytic approaches, because the entire solar spectrum is utilized, as opposed to only using the high energy portion of the spectrum which is capable of splitting chemical bonds directly. The overall efficiency of a solar thermochemical reactor is constrained by a steady state balance between the power density of the fuel output and solar energy input. The energy conversion process from sunlight to chemical energy can be divided into two distinct conversions, namely (1) solar to thermal energy conversion, and (2) thermal to chemical energy conversion. To reach the high temperatures required for the reduction step, concentrated solar radiation is usually trapped in a cavity after entering through a small aperture to minimize reradiation losses. The walls and any structures contained inside the cavity serve as the solar receiver, which absorbs the sunlight and converts it to thermal energy. The thermal energy is then converted to chemical energy in the form of fuel (i.e., via a partial redox cycle) in what we will refer to in the subsequent analysis as the reactor. (Yuan et al., 2015)

This article develops some of the underlying science and describes some of the latest technological developments for achieving this goal. The reader is first introduced to the principles of solar energy concentration and to the thermodynamics of solar thermochemical conversion. State of the art reactors are described as well as the most promising solar thermochemical processes. (Abedin, 2011)

Solar Collector Applications

Solar collectors have been used in a variety of applications.

These are described in this section. The most important technologies in use are listed together with the type of collector that can be used in each case.

Solar Water Heating system

In solar water heating systems, potable water can either be heated directly in the collector (direct systems) or indirectly by a heat transfer fluid that is heated in the collector, passes through a heat exchanger to transfer its heat to the domestic or service water (indirect systems). The heat transfer fluid is transported either naturally (passive systems) or by forced circulation (active systems).

(Yuan et al., 2015)

Thermo syphon systems (passive)

Thermo syphon systems, heat potable water or heat transfer fluid is use natural convection to transport it from the collector to storage. The water in the collector expands becoming less dense as the sun heats it and rises through the collector into the top of the storage tank. The main disadvantage of thermo syphon systems is the fact that they are comparatively tall units, which makes them not very attractive aesthetically. Additionally, extremely hard or acidic water can cause scale deposits that clog or corrode the absorber fluid passages. For direct systems, pressure reducing valves are required when the city water is used directly (no cold water storage tank) and pressure is greater than the working pressure of the collectors. (Ermanoski & Siegel, 2014)

Integrated collector storage systems (passive)

ICS systems use hot water storage as part of the collector, i.e. the surface of the storage tank is used also as an absorber. As in all other systems, to improve stratification, the hot water is drawn from the top of the tank and cold make-up water enters to the bottom of the tank on the opposite side. The main disadvantage of the ICS systems is the high thermal losses from the storage tank to the surroundings since most of the surface area of the storage tank cannot be thermally insulated as it is intentionally exposed for the absorption of solar radiation. (Behera et al., 2019)

Solar thermal power systems

The process of conversion of solar to mechanical and electrical energy by thermal means is fundamentally similar to the traditional thermal processes. These systems differ from the ones considered so far as these operate at much higher temperatures. This section is concerned with generation of mechanical and electrical energy from solar energy by processes based mainly on concentrating collectors and heat engines. Identifying the best available sites for the erection of solar thermal power plants is a basic issue of project development. (Ranjan et al., 2017)

Parabolic dish systems

A parabolic dish concentrates solar energy onto a receiver at its focal point. The receiver absorbs the energy and converts it into thermal energy. This can be used directly as heat or supply for power generation. The thermal energy can either be transported to a central generator for conversion, or it can be converted directly into electricity at a local generator coupled to the receiver. (Athari et al., 2017)

LITERATURE REVIEW

(Jarimi et al., 2019) presents a literature survey and a review that add insights into the current state-of-the-art THS technologies, covering: the THS materials, THS reactor design

and THS as thermal batteries. Emphasis is placed on THS for solar thermal energy storage and also for industrial waste heat recovery. At the materials level, in addition to a review on THS material sorbents, emphasis is placed on innovative composite THS materials with salt mixtures and metal-organic frameworks materials. Reactor design is one of the major fields of THS system development. In this paper, we also review several types of innovative reactor designs, including hybrid THS systems, towards obtaining advanced reactor concept, numerical studies in THS studies mainly covering the heat and mass transfer in the reactor designs, and also the implementation of THS systems as thermal batteries.

(Huang et al., 2018) introduces a heavily biased and robust iron-based $\text{La}_{0.6}\text{Sr}_{0.4}\text{Fe}_{0.8}\text{Al}_{1.2}\text{O}_{3-\delta}$ oxygen carrier for syngas processing via a thermochemical process powered by solar energy. It is observed that during redox cycling a complex structural transition occurs between the perovskite layer and a core – shell composite of FeO@oxides . The layer of oxide, acting as a micromembrane, avoids direct interaction between methane and fresh iron (0), and inhibits coke deposition. This core – shell intermediate is either regenerated in oxygen or more specifically in oxidant pure water – Carbon dioxide with parallel production of another source of syngas to the initial perovskite structure. Doping with aluminium oxides decreases the ground oxygen content by reducing free electrons in the perovskite matrix, while preventing over oxidation of methane. As a result, this material exhibits high stability with carbon monoxide selectivity above 95% and yielding an ideal syngas of H_2/CO ratio of 2/1.

(Zhang et al., 2018) explains that thermal transfer and fluid flow characteristics have important impacts on the performance of hydrogen output as a primary technological parameter for porous media solar thermochemical reactor. The implementation of computational fluid dynamics (CFD) could solve these problems more effectively and at a lower cost. Additionally, the option of various models of thermal transport may cause results to vary. In this research, the thermal transport and fluid flow characteristics of solar thermochemical reactor with high-temperature porous media were investigated using FLUENT user-defined functions (UDFs) software with different thermo physical models. The findings suggest that the local thermal non-equilibrium model (LTNE) and radioactive transfer model have been shown to be invaluable for the thermal efficiency study of a thermochemical reaction system with high working temperatures. In comparison, Wu model of momentum source is best suited for simulating energy, while Wu model and Vafai model of heat transfer display no variation in temperature distribution.

(Rao & Dey, 2017) discussed that solar photochemical potential of splitting water (artificial photosynthesis) to generate hydrogen is rising as a workable process. The photo voltaic thermochemical route additionally guarantees to be an attractive capability of accomplishing this objective. In this paper we existing one of a kind kinds of thermochemical cycles that one can use for the purpose. These encompass the low-temperature multistep system as nicely as the high-temperature two-step process. It is noteworthy that the multistep manner primarily based on the Mn (II)/Mn (III) oxide machine can be carried out at 700 °C or 750 °C. The two-step technique has been finished at 1,300 °C/900 °C by

way of the usage of yttrium-based uncommon earth manganite. It appears viable to render this high-temperature method as an isothermal process. Thermodynamics and kinetics of H₂O splitting are mostly managed by using the inherent redox properties of the materials.

(Guene Lougou et al., 2017) This paper investigated radiation heat transfer and temperature distributions of solar thermochemical reactor for syngas production using the finite volume discrete ordinate method (fvDOM) and P1 approximation for radiation heat transfer. Different parameters including absorptivity, emissivity, and reflection based radiation scattering, and carrier gas flow inlet velocity that would greatly affect the reactor thermal performance were sufficiently investigated. The fvDOM approximation was used to obtain the radiation intensity distribution along the reactor. The drop in the temperature resulted from the radiation scattering was further investigated using the P1 approximation. The results indicated that the reactor temperature difference between the P1 approximation and the fvDOM radiation model was very close under different operating conditions. However, a big temperature difference which increased with an increase in the radiation emissivity due to the thermal non-equilibrium was observed in the radiation inlet region. It was found that the incident radiation flux distribution had a strong impact on the temperature distribution throughout the reactor. This paper revealed that the temperature drop caused by the boundary radiation heat loss should not be neglected for the thermal performance analysis of solar thermochemical reactor.

(Abdiwe & Haider, 2016) said that the thermochemical system the usage of ammonia as strength storage service is investigated in this study. A mathematical model used to be developed to predict the conduct of each reactor in the ammonia-based closed-loop system. For the significance of the dissociation and formation system in the system, the mannequin centered solely on the photo voltaic and the synthesis reactors. The learn about indicates that retaining the fantastic mass waft price is necessary for reaching the most ammonia dissociation and formation procedures and as an end result the most thermal output. Operating the react- tors at greater strain than cautioned will increase the formation of ammonia at the synthesis; however, it lowers the thermal output of the system.

(Bellan et al., 2014) analyzed that a lab-scale thermochemical reactor is structured and manufactured for the solar-driven warm decrease of non-unstable manganese oxide to create hydrogen by water parting thermo synthetic cycles. A period subordinate three dimensional mathematical model is created to examine the presentation of the reactor since the synthetic energy unequivocally relies upon irradiance, temperature and liquid stream conveyance around the reactant. Radiation heat transfer is determined by utilizing surface-to-surface (S2S) radiation model. Thermo-liquid stream, assimilation effectiveness and the temperature appropriation of the example are anticipated as a component of time and the model is approved by exploratory estimations.

(Ermanoski & Siegel, 2014) reported on results with respect to the yearly normal productivity of a recovering pressed molecule bed reactor for solar-thermochemical hydrogen creation through a two-advance metal oxide cycle, utilizing point by point mathematical models. The key discoveries are

that reactor effectiveness is generously level as an element of direct ordinary irradiance, prompting a yearly normal proficiency practically equivalent to the structure point productivity, and that sufficient top notch squander heat is accessible to make independent activity plausible, including feedstock water creation. This end has extensive ramifications for solar-thermochemical hydrogen and fuel creation when all is said in done.

(Lipiński et al., 2013b) reported outlines of the advances, obstacles and possibilities in heat transfer research as applied to thermochemical high-temperature systems using high-flow solar irradiation as the source of process heat. Listed related fields such as radiative spectroscopy and the heat and mass characterization of heterogeneous media dependent on tomography, Hightemperature kinetics Heterogeneous reactions, heat and mass transfer simulation of solar thermochemical processes, and thermal measurements in high-temperature processes are discussed, with brief description of their methods and descriptions of the effects of selected applications.

METHODOLOGY

1. Design and modeling of porous media solar thermochemical reactor in NX 11 according to the model requirement and literature survey.
2. Further converting the NX 11 File in .STEP format for importing it in ANSYS Fluent work bench.
3. Assigning the name selection to the different parts of thermochemical reactor model.
4. Meshing of thermochemical reactor model for performing the simulation process.
5. Providing the suitable boundary conditions according to the selected base paper.
6. Assigning the material properties to the model.
7. Setting the proper setup for CFD analysis procedure.
8. Evaluating the results after the finish of simulation work.

Meshing

Meshing is an integral part of the CAE simulation method. The mesh affects the accuracy, convergence and speed of the solution. Furthermore, the time it takes to create and mesh a version is often a good sized part of the time it takes to get consequences from a CAE solution. Therefore, the higher and extra automated the meshing equipment, the better the solution.

The following number of nodes and element are generated in meshing,

Table 1 Nodes and element

Nodes	Elements
80785	79635

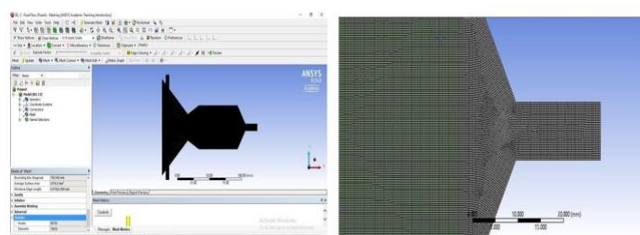


Figure 0.1 Mesh with enlarged image

Boundary Condition

Assigning the name selection to the of tube, providing the suitable boundary condition at inlet velocity is 0.005m/s and inlet solar temperature is 1600 K. The outlet walled is cooled at constant temperature 600 K., materials properties are assigned, and the material property is shown in below table. There are two material is used which are Silicon carbide and air. The solar thermochemical reactor contained silicon carbide porous medium and air is used as a heat transfer fluid.

Table 2 Material Property

Material	SIC (Silicon Carbide)	Air
Density (Kg/m3)	3100	1.225
Thermal Conductivity (W/m2K)	120	0.0242
Specific Heat (J/Kg.K)	750	1006.43

RESULT

Result for selecting porosity

The solar thermochemical reactor consists of a chemical reactor for which three cases are taken to select the porosity of the material. Three cases with constant velocity and same length of porous media are taken in which the porosity is increased by 10% in every case is shown in table.

Table 3 Cases for selecting porosity

	Porosity	Velocity (m/s)	Length of porous Media (mm)
Case 1	0.7	0.005	60
Case 2	0.8	0.005	60
Case 3	0.9	0.005	6

To select the porosity of the material, temperature is one of the main parameter to be considered. Following are the results of three cases temperature contour.

Case 1- The temperature contour for case 1 is shown in the figure 2. Various colors in the figure shows different temperature range such as orange color indicates the maximum temperature and blue color shows the minimum temperature.

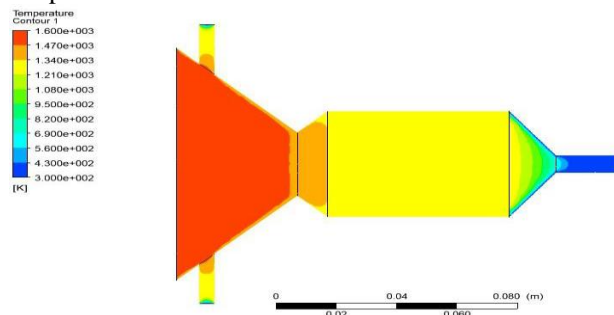


Figure 2 Temperature contour for Case 1

Case 2- The temperature contour for case 2 is shown in the figure 3. Various colours in the figure shows different temperature range such as orange color indicates the

maximum temperature and blue color shows the minimum temperature.

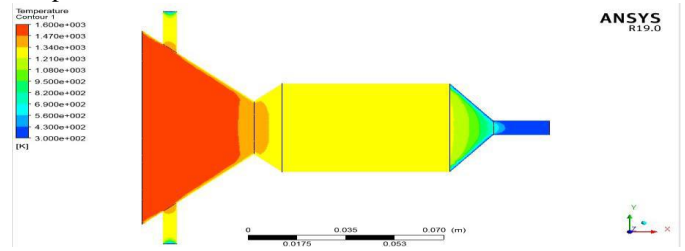


Figure 3 Temperature contour for Case 2

Case 3- The temperature contour for case 3 is shown in the figure 4. Various colors in the figure shows different temperature range such as orange color indicates the maximum temperature and blue color shows the minimum temperature.

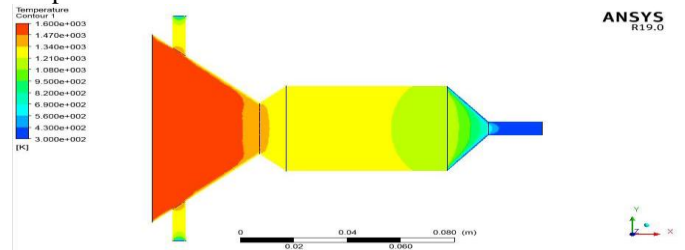


Figure 4 Temperature contour for Case 3 Temperature comparisons

The graph show that while increasing the porosity the temperature decreases. The porous medium at a length of 0.05 to 0.1 meter remained quite stable. This change in temperature is produced because high porous material of alloy has to move gas in large quantity in porous contact zone. Case 3 will be ideal for the chemical reactor as its temperature is lowest when the length is increased.

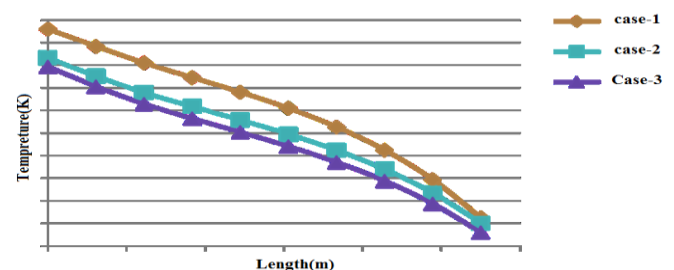


Figure 5 Graph representing variations in temperature when length changed Pressure comparisons

When length of the porous material is increased, the pressure decreases. In the table given below, it is clear that in each case the pressure is decreasing as the length of porous mode is increasing.

With the increase of length of material the pressure decreases, shown by a graph in figure 6.

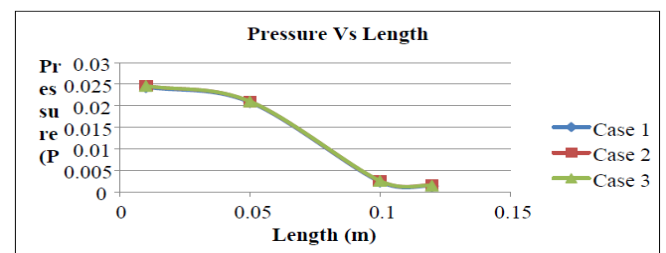


Figure 6 : Graph represents Pressure v/s Length

Result for selecting Velocity

The solar thermochemical reactor consists of a chemical reactor for which earlier three cases were taken to select the porosity. Now two cases will be taken to select the velocity. Best result porosity will be taken as porosity in case 4 and case 5. The length of the porous media will also remain constant. To select the velocity, velocity will be varied as shown in table 4.3.

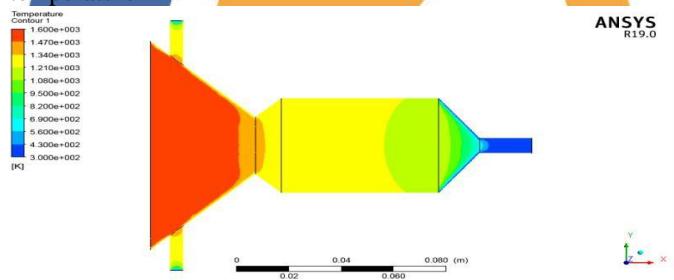
Table 4 Cases for selecting velocity

	Porosity	Velocity (m/s)	Length of porous Media (mm)
Case 4	0.9	0.09	60
Case 5	0.9	0.002	60

Temperature

To select the velocity of the material, temperature is one of the main parameter to be considered. And while increasing the material the temperature should decrease maximum. Following are the results of two cases; Case 4 and Case 5 temperature contour.

Case 4- The temperature contour for case 4 is shown in the figure 7. Various colors in the figure shows different temperature range such as orange color indicates the maximum temperature and blue color shows the minimum temperature



Heat transfer rate

To select the velocity, the heat transfer rate of Case 4 and Case 5 are shown in figure 9. It is clear from the figure that heat transfer of Case 4 is 4818.583 and heat transfer rate of Case 5 is 4818.388. Heat transfer rate of Case 4 is higher than Case 5 from the results shown in the graph.

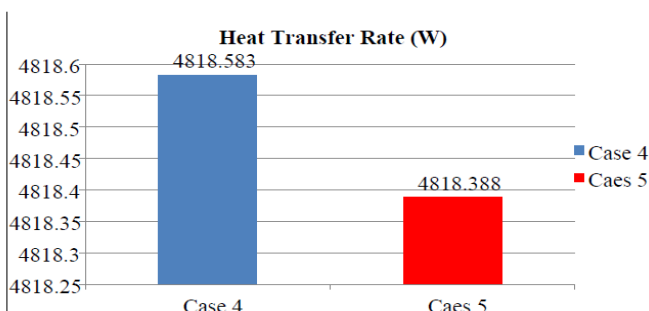


Figure 9 Graph representing Heat Transfer Rate

Temperature comparisons

The graph show that when length of the material is increased, the temperature decreased. The temperature decrease is same in both the cases.

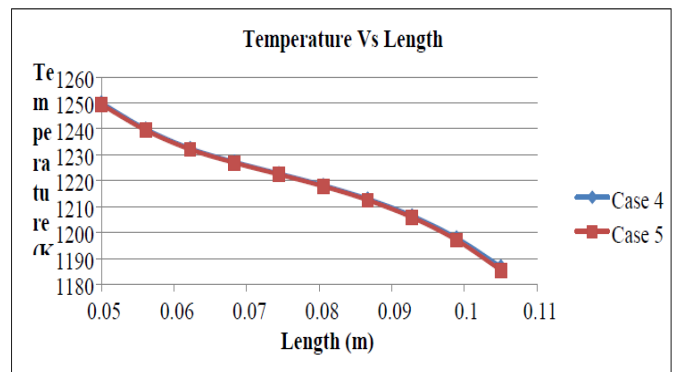


Figure 10 Representing temperature comparison

Result for selecting Length

The solar thermochemical reactor consists of a chemical reactor for which five cases were taken earlier. Now two cases, Case 6 and Case 7 will be taken to select the length of the material. The cases with constant velocity and porosity are taken in which the length of porous material is different for both cases as shown in the table:

Table 5 Cases for selecting length

	Porosity	Velocity (m/s)	Length of porous Media (mm)
Case 6	0.9	0.002	50
Case 7	0.9	0.002	70

Temperature

To select the length of the material, temperature is one of the main parameter to be considered. Following are the results of temperature contour of two cases.

Case 6- The temperature contour for case 6 is shown in the figure 11. Various colors in the figure shows different temperature range such as orange color indicates the maximum temperature and blue color shows the minimum temperature.

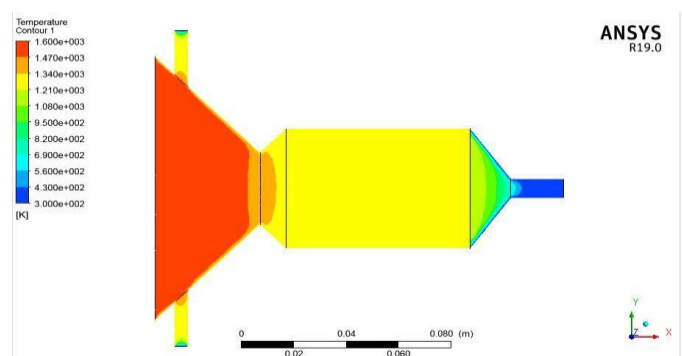


Figure 11 Temperature contour for Case 6

Case 7- The temperature contour for case 7 is shown in the figure 12. Various colors in the figure shows different temperature range such as orange color indicates the maximum temperature and blue color shows the minimum temperature.

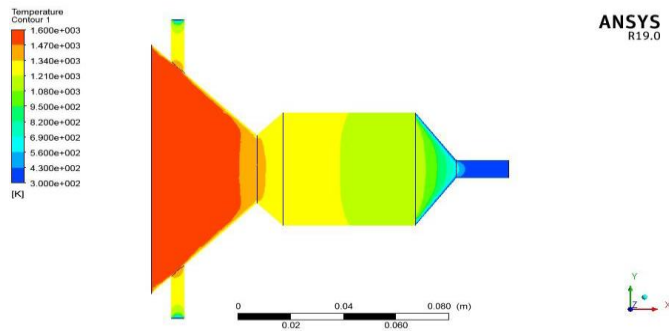


Figure 12 Temperature contour for Case 7

Heat transfer rate comparisons

To select the length, the heat transfer rate of Case 6 and Case 7 are shown in figure 13. It is clear from the figure that heat transfer of Case 6 is 4410.123 and heat transfer rate of Case 7 is 4901.343. Heat transfer rate of Case 7 is higher than Case 6 from the results shown in the graph

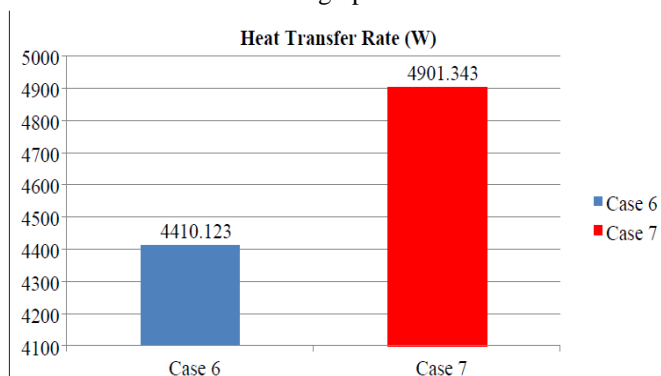


Figure 13 graph showing heat transfer rate Temperature comparison

The graph show that when length of the material is increased, the temperature decreased. The temperature decrease is different in both the cases. The maximum temperature decrease is done by Case 7 in comparison to Case 6.

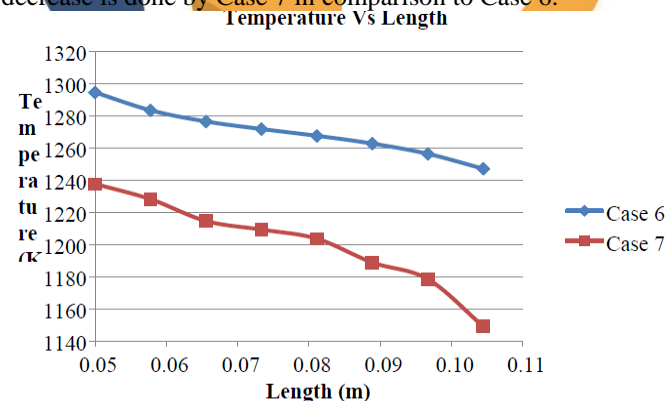


Figure 14 graph showing temperature comparison with respect to length

Overall Heat Transfer Comparisons

The heat transfer rate of all the cases is shown in the figure 15 given below. It is the comparison of all the parameters such as porosity, velocity and length of the porous media with respect to heat transfer comparison. Case 1 shows the least heat transfer rate, its value is 3721.077W. While Case 7 shows the highest Heat Transfer Rate which is 4901.343W.

Overall Temperature

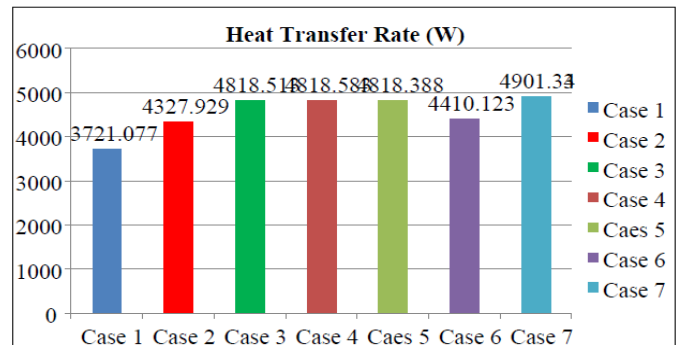


Figure 15 Graph showing Overall Heat Transfer Rate

Overall Temperature Comparisons

The temperature comparison of all the cases is shown in the figure 16 given below. It is the comparison of all the parameters such as porosity, velocity and length of the porous media with respect to temperature. Case 3 shows the least value of temperature when the length increased which is required by the chemical reactor.

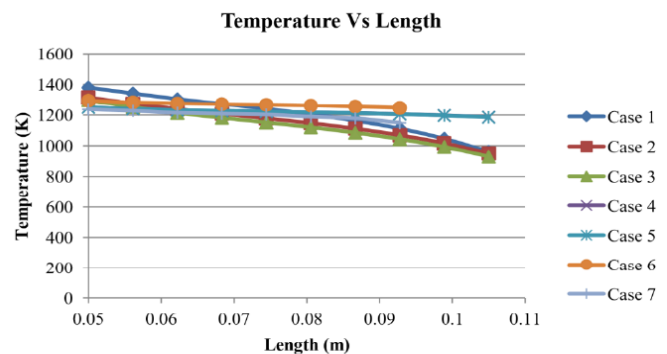


Figure 16 Graph showing Overall Temperature Comparison Average Temperature Comparisons

The graph given below shows the different temperatures. Here the average of each case is given, from which it can be concluded that Case 1 and Case 4 are showing the maximum average temperature which is also same i.e. 1327.64K. And case 6 shows the least value 1205.24K of average temperature.

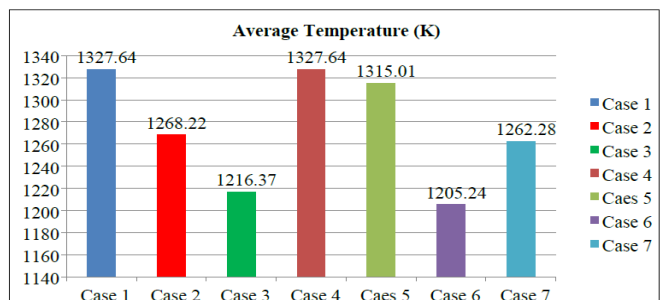


Figure 17 Average temperature comparison graph

CONCLUSION

Solar thermochemical processes make use of concentrated solar radiation for driving chemical reactions. The processes are classified into those for production of solar fuels and chemical commodities. Heat and mass transfer characterization of heterogeneous reacting media, formulation of accurate kinetic rate equations, modeling of combined heat and mass transfer in heterogeneous reacting media, and accurate measurements of radiative fluxes and temperatures in high-temperature reacting systems are of fundamental

importance for advancements of solar thermochemical reactor technology for efficient solar thermochemical energy conversion. The concept described above provides several advantages by varying different parameters to increase the efficiency of solar thermochemical reactor. To increase the length of porous media in a chemical reactor, seven cases were taken. The conclusions obtained from these cases are discussed below:

- While increasing the porosity, the temperature decreases and the porosity of 0.9 shows the best results and other parameters remained constant.
- While varying the velocity in two of the above cases, it can be concluded that less velocity gives better results.
- The overall comparison of heat transfer, temperature and average temperature are also calculated. Case 7 shows the highest Heat Transfer Rate i.e. 4901.343W, Case 3 shows the least value of temperature when the length increased i.e. 900K; Case 1 and Case 4 are showing the maximum average temperature i.e. 1327.64K.

Parameters like heat transfer rate, pressure, velocity and temperature are observed in it. Efficiency, heat flux and many other parameters can be considered in further studies.

REFERENCES

- Abdiwe, R. A., & Haider, M. (2016). A mathematical model for ammonia solar and synthesis reactors. *Renewables: Wind, Water, and Solar*, 3(1), 12. <https://doi.org/10.1186/s40807-016-0034-4>
- Abedin, A. H. (2011). A Critical Review of Thermochemical Energy Storage Systems. *The Open Renewable Energy Journal*, 4(1), 42–46. <https://doi.org/10.2174/1876387101004010042>
- Athari, M. H., Wang, Z., & Eylas, S. H. (2017). Time-series analysis of photovoltaic distributed generation impacts on a local distributed network. 2017 IEEE Manchester PowerTech, Powertech 2017. <https://doi.org/10.1109/PTC.2017.7980908>
- Behera, S., Kumar, B., & Behera, R. K. (2019). Minimization of Input Ripple Current for Soft-Switching Buck-Boost Converter. *International Journal of Engineering and Advanced Technology*, 9(2), 1174–1181. <https://doi.org/10.35940/ijeat.b3524.129219>
- Bellan, S., Alonso, E., Perez-Rabago, C., Gonzalez-Aguilar, J., & Romero, M. (2014). Numerical modeling of solar thermochemical reactor for kinetic analysis. *Energy Procedia*, 49, 735–742. <https://doi.org/10.1016/j.egypro.2014.03.079>
- Ermanoski, I., & Siegel, N. (2014). Annual average efficiency of a solar-thermochemical reactor. *Energy Procedia*, 49, 1932–1939. <https://doi.org/10.1016/j.egypro.2014.03.205>
- Guene Lougou, B., Shuai, Y., Chen, X., Yuan, Y., Tan, H., & Xing, H. (2017). Analysis of radiation heat transfer and temperature distributions of solar thermochemical reactor for syngas production. *Frontiers in Energy*, 11(4), 480–492. <https://doi.org/10.1007/s11708-017-0506-2>
- Huang, C., Wu, J., Chen, Y. T., Tian, M., Rykov, A. I., Hou, B., Lin, J., Chang, C. R., Pan, X., Wang, J., Wang, A., & Wang, X. (2018). In situ encapsulation of iron(0) for solar thermochemical syngas production over iron-based perovskite material. *Communications Chemistry*, 1(1), 2–11. <https://doi.org/10.1038/s42004-018-0050-y>
- Abdiwe, R. A., & Haider, M. (2016). A mathematical model for ammonia solar and synthesis reactors. *Renewables: Wind, Water, and Solar*, 3(1), 12. <https://doi.org/10.1186/s40807-016-0034-4>
- Abedin, A. H. (2011). A Critical Review of Thermochemical Energy Storage Systems. *The Open Renewable Energy Journal*, 4(1), 42–46. <https://doi.org/10.2174/1876387101004010042>
- Athari, M. H., Wang, Z., & Eylas, S. H. (2017). Time-series analysis of photovoltaic distributed generation impacts on a local distributed network. 2017 IEEE Manchester PowerTech, Powertech 2017. <https://doi.org/10.1109/PTC.2017.7980908>
- Behera, S., Kumar, B., & Behera, R. K. (2019). Minimization of Input Ripple Current for Soft-Switching Buck-Boost Converter. *International Journal of Engineering and Advanced Technology*, 9(2), 1174–1181. <https://doi.org/10.35940/ijeat.b3524.129219>
- Bellan, S., Alonso, E., Perez-Rabago, C., Gonzalez-Aguilar, J., & Romero, M. (2014). Numerical modeling of solar thermochemical reactor for kinetic analysis. *Energy Procedia*, 49, 735–742. <https://doi.org/10.1016/j.egypro.2014.03.079>
- Ermanoski, I., & Siegel, N. (2014). Annual average efficiency of a solar-thermochemical reactor. *Energy Procedia*, 49, 1932–1939. <https://doi.org/10.1016/j.egypro.2014.03.205>
- Guene Lougou, B., Shuai, Y., Chen, X., Yuan, Y., Tan, H., & Xing, H. (2017). Analysis of radiation heat transfer and temperature distributions of solar thermochemical reactor for syngas production. *Frontiers in Energy*, 11(4), 480–492. <https://doi.org/10.1007/s11708-017-0506-2>
- Huang, C., Wu, J., Chen, Y. T., Tian, M., Rykov, A. I., Hou, B., Lin, J., Chang, C. R., Pan, X., Wang, J., Wang, A., & Wang, X. (2018). In situ encapsulation of iron(0) for solar thermochemical syngas production over iron-based perovskite material. *Communications Chemistry*, 1(1), 2–11. <https://doi.org/10.1038/s42004-018-0050-y>